

Equilibrium properties and force-driven unfolding pathways of RNA molecules

A. Imparato*

*Department of Physics and Astronomy, University of Aarhus,
Ny Munkegade, Building 1520, DK-8000 Aarhus C, Denmark*

A. Pelizzola†

*Dipartimento di Fisica and CNISM, Politecnico di Torino, c. Duca degli Abruzzi 24, Torino, Italy and
INFN, Sezione di Torino, Torino, Italy*

M. Zamparo‡

Dipartimento di Fisica and CNISM, Politecnico di Torino, c. Duca degli Abruzzi 24, Torino, Italy

The mechanical unfolding of a simple RNA hairpin and of a 236-bases portion of the Tetrahymena thermophila ribozyme is studied by means of an Ising-like model. Phase diagrams and free energy landscapes are computed exactly and suggest a simple two-state behaviour for the hairpin and the presence of intermediate states for the ribozyme. Nonequilibrium simulations give the possible unfolding pathways for the ribozyme, and the dominant pathway corresponds to the experimentally observed one.

PACS numbers: 87.15.A-; 87.15.Cc; 87.15.La

The study of the RNA three-dimensional structure has received a boost by the recent discovery that some RNA molecules act as enzymes in several key cellular processes in complete absence of protein cofactors [1].

As for proteins, the shape of RNA molecules is strictly connected to their function, and thus the study of the response to external forces helps to understand how biomolecules transform mechanical inputs into chemical signals. Recent experiments and simulations have shown how it is possible to extract information on the RNA structure by using force spectroscopy, where RNA molecules are manipulated by using controlled forces.

In particular, remarkable experimental works [2, 3] have investigated the connections between the molecular structure of RNA hairpins and Tetrahymena thermophila ribozyme, and the respective unfolding pathways under mechanical stress.

Motivated by such experiments, several groups have proposed theoretical and numerical approaches to the mechanical unfolding of RNA molecules [4, 5, 6, 7, 8]. In particular, by using a coarse-grained Gō-model and Molecular Dynamics (MD) simulations, Thirumalai and coworkers have computed phase diagrams and free energy landscapes of RNA hairpins [5, 8], and the unfolding pathways of larger, more complex RNA molecules [6, 7].

However, MD simulations are computationally demanding, and even in the simple case of the determination of the phase diagram, simulations have to be restarted for every choice of the model parameters. Here we introduce a simple discrete model for RNA molecules under external force, whose thermodynamics is exactly solvable, and as such is able to provide exact thermodynamical results for any size of the molecules, in a computation time which is incomparably smaller than the time needed for simulations. We exploit this model to

obtain the force-temperature (f, T) phase diagram of a small and a large RNA molecule and their free energy landscape as a function of the molecular elongation.

Furthermore, by using Monte Carlo simulations (MC), we investigate the unfolding pathways of the larger molecule, finding that the most probable path from the native to the unfolded state agrees with the experimentally determined one. It is worth noting that the present model has been used to evaluate the phase diagram, the free energy landscape [9], and the unfolding pathways [10] of widely studied proteins, showing a good degree of agreement with the corresponding experimental results.

The model – We use a Gō model defined by the energy

$$H(m, \sigma) = - \sum_{i=1}^{N-1} \sum_{j=i}^N \epsilon_{ij} \Delta_{ij} \prod_{k=i}^j m_k - fL, \quad (1)$$

where $L = \sum_{i \leq j} l_{ij} \sigma_{ij} (1 - m_{i-1})(1 - m_j) \prod_{k=i}^{j-1} m_k$ is the end-to-end length of the molecule and $m_k = 0, 1$ is associated to the covalent bond between bases k and $k + 1$. $m_k = 1$ (respectively 0) means that this bond is (resp. is not) in a native-like state. Given the state of the m variables, for an RNA molecule with $N + 1$ bases, $n_\sigma(m) = 1 + \sum_{k=1}^N (1 - m_k)$ orientational degrees of freedom are introduced. Such degrees of freedom, σ_{ij} , describe the orientation of the $n_\sigma(m)$ native-like stretches, relative to the external force f . Indeed, if a native-like stretch extends from base i to base $j \geq i$, then $(1 - m_{i-1})(1 - m_j) \prod_{k=i}^{j-1} m_k = 1$. Such a stretch can be as short as a single base $i = j$. We set as boundary conditions $m_0 = m_{N+1} = 0$. The orientation σ_{ij} of a native-like stretch is also a binary variable: $\sigma_{ij} = +1$ (respectively -1) represents a stretch oriented parallel (resp. antiparallel) to the external force f . l_{ij} is the length of the $i - j$ native stretch, taken from the Protein Data Base

(PDB) and defined as the distance between the phosphorus atoms of bases i and $j + 1$. Δ_{ij} is the element of the contact matrix, which takes the value 1 if the bases i and $j + 1$ are in contact, and 0 otherwise. Within the present model, bases i and $j + 1$ are considered to be in contact if at least two atoms, one from each base, are closer than $\delta = 4$ Å. Finally ϵ_{ij} is the corresponding interaction strength, which is proportional to the number of atom pairs, which are in contact according to the above criterion. We have shown [9] that, as far as the equilibrium thermodynamics is concerned, the sum over the σ variables can be performed exactly, and in the $f = 0$ case a well-known Ising-like model of protein folding is obtained [11]. Stacking interactions are implicitly taken into account in the present model: one can easily check that, for instance, the formation of a contact between bases $i + 1$ and $j - 1$ (if present in the native structure) is a necessary condition for the formation of an $i - j$ native contact.

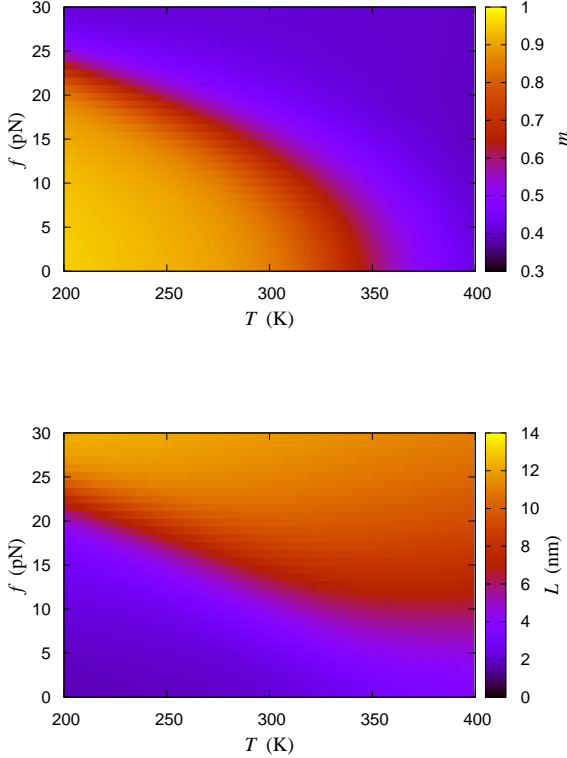


Figure 1: (Color online) Force-Temperature phase diagrams of the 1EOR molecule. Upper panel: average order parameter $\langle m \rangle$. Lower panel: average end-to-end length $\langle L \rangle$.

Simple hairpin (P5GA) – We first consider a 22-nucleotides RNA hairpin, (PDB code 1EOR, see ref.[12] for the secondary structure), which is similar to the P5ab in the P5abc domain of group I intron [2]. We first focus on the equilibrium properties of the molecule, and then

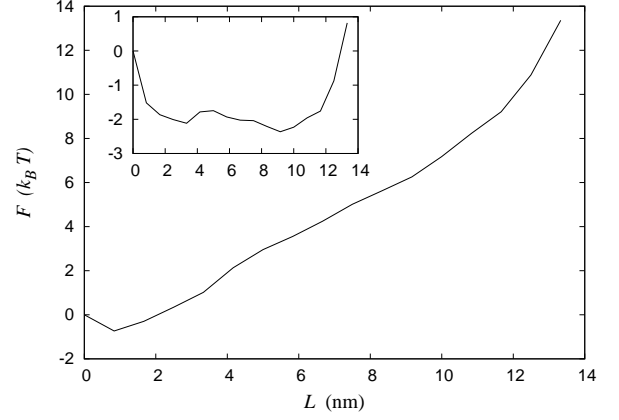


Figure 2: Free energy landscape F_0 of the 1EOR molecule as a function of the molecular elongation L . Inset, tilted FEL $F_0 - fL$, with $f = 15.4$ pN.

study the unfolding kinetics induced by external forces.

In fig. 1, the (f, T) phase diagrams are plotted. They show that P5GA behaves like a two-state system, the transition region from the folded to the unfolded state being quite narrow. It is also in good agreement with that by Hyeon and Thirumalai [5] for the same molecule.

An interesting quantity that characterizes the stability of a biopolymer, is the free energy landscape (FEL) F_0 as a function of its end-to-end elongation L , defined as

$$F_0(L) = -k_B T \ln \left[\sum_x e^{-\beta H_0(x)} \delta(L(x) - L) \right], \quad (2)$$

where x is the microscopic state of the system, and the sum is restricted to those states, whose value of the macroscopic variable $L(x)$ is equal to the argument L of F_0 . Here $H_0(x)$ corresponds to the hamiltonian (1) with $f = 0$. As discussed in [9], $F_0(L)$ can be exactly computed in the present model. The landscape is plotted in fig. 2, for $T = 300$ K. When an external constant force f is applied to the molecule free ends, one gets the tilted landscape $F(L, f) = F_0(L) - fL$, which is plotted in fig. 2, for $f = 15.4$ pN. From the phase diagram in fig. 1 one sees that for this value of the force, the molecule length is about half of its maximum value $L_{\max} \simeq 13.8$ nm. At the same time, the FEL exhibits two wells at small and large elongation, indicating that the molecule hops from the folded to the unfolded state, for this value of the force [5]. The FEL of the same molecule was obtained in [5, 7, 8] by using an off-lattice coarse grained model and MD simulations. In these papers, $F(L, f)$ was estimated by analyzing the kinetics of the molecule under force, i.e., by sampling the occupation frequency of those states with a given elongation L . This method is expected to give reliable results only for small molecules, like the one at issue, where the phase space of the molecule is sampled according to its equilibrium phase space distribution. In the case of larger

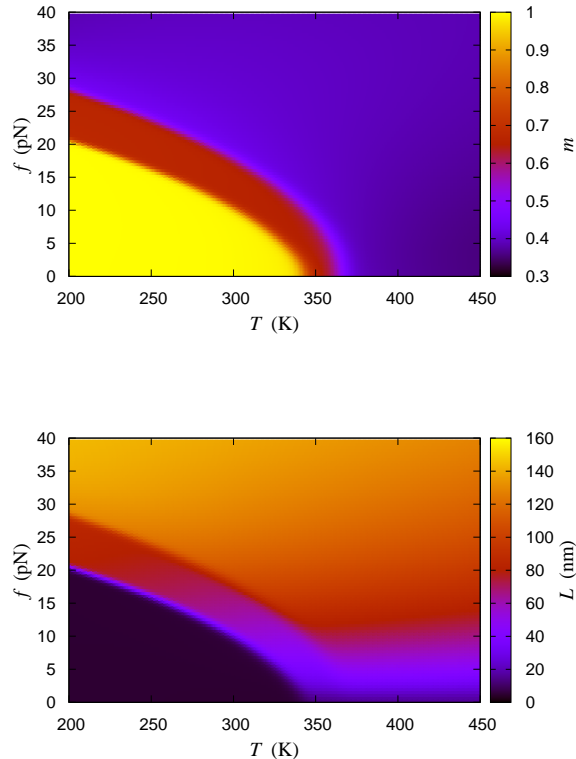


Figure 3: (Color online) Force-Temperature phase diagrams of the *T. thermophila* ribozyme. Upper panel: average order parameter $\langle m \rangle$. Lower panel: average end-to-end length $\langle L \rangle$.

molecules, at small forces, one expects that the states with large L are not sampled with the correct frequency, as computer simulations usually fail to visit rare states. On the contrary, the phase diagrams and landscapes, as given by the present model, are exact results, and can be obtained for any molecule size and any value of f and T .

Tetrahymena thermophila ribozyme (1GRZ) – In the following we investigate the thermodynamical equilibrium properties and the mechanical unfolding of the *Tetrahymena thermophila* ribozyme [13], PDB code 1GRZ, whose mechanical unfolding has been studied both experimentally [3] and with computational techniques [6]. We consider the structured part from base 96 to 331, which exhibits several secondary structure elements (SSE), named P_n with $n=3, \dots, 9$, see ref. [12].

In fig. 3 we plot the (f, T) phase diagram of the 1GRZ molecule. At variance with the case of the hairpin, this larger molecule exhibits a wider transition region, reflecting the presence of intermediate states along the unfolding pathway, as will be discussed in detail below.

In fig. 4, we plot the unperturbed FEL F_0 as a function of the end-to-end length L at $T = 300$ K. In the same figure, we plot the tilted FEL $F(L, f)$ for two values of the external force $f = 8.82, 17.64$ pN. From the

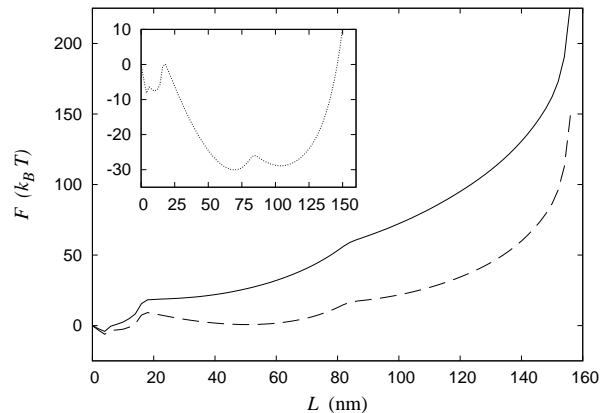


Figure 4: Free energy landscape F_0 of the 1GRZ molecule as a function of the molecular elongation L , for $T = 300$ K (full line). Tilted FEL $F(L, f)$ for two values of the force $f = 8.82$ pN (dashed line) and $f = 17.64$ pN (dotted line, inset).

phase diagram in fig. 3 one sees that for $f = 17.64$ and $T = 300$ K, the average end-to-end length is half of its maximum value $L_{\max} \simeq 155$ nm. The FEL at $f = 17.64$ pN exhibits two major and one minor energy wells, indicating the coexistence of three states characterized by three different values of L for this force.

In order to study the mechanical unfolding of the ribozyme, we consider here the experimental protocol where the external force is applied by tethering the molecule to a colloidal particle trapped in an optical trap: $f(t) = k(X(t) - L(t))$, where $L(t)$ is the end-to end length of the molecule at time t , while k and $X(t) = r \cdot t$ are the stiffness and the center of the trap, respectively. This experimental setup corresponds to that used in ref. [3], which we will use as a reference to compare our results.

In ref. [10], the present model was used to trace the state of SSEs of a protein. Similarly, one can monitor the unfolding of a single SSE of 1GRZ by considering a suitable order parameter for each SSE. Here we choose the fraction of native contacts within an element. The order parameter of the SSE P_n will be defined as $\phi_{P_n} = \sum'_{ij} \Delta_{ij} \prod_{k=i}^j m_k / N_{P_n}$, where the prime means that i and j run over those bases belonging to P_n , and $N_{P_n} = \sum'_{ij} \Delta_{ij}$ is the total number of native contacts in P_n . This approach allows us to trace the current state of each SSE. The unfolding time of a given SSE is defined as the time at which the corresponding order parameter crosses a given threshold $\phi_u = 1/3$ for the first time [10].

In order to find the typical unfolding pathways, we consider 1000 trajectories, simulated with a standard Monte Carlo algorithm [9], where the trap stiffness and the velocity take the values $k = 13$ pN/nm, and $r = 0.36$ nm/(MC Step). Time is a discrete variable counting the number of MC steps. A typical trajectory is plotted in fig. 5. In the force-extension curve unfolding peaks can be observed. By comparing the position of the peaks

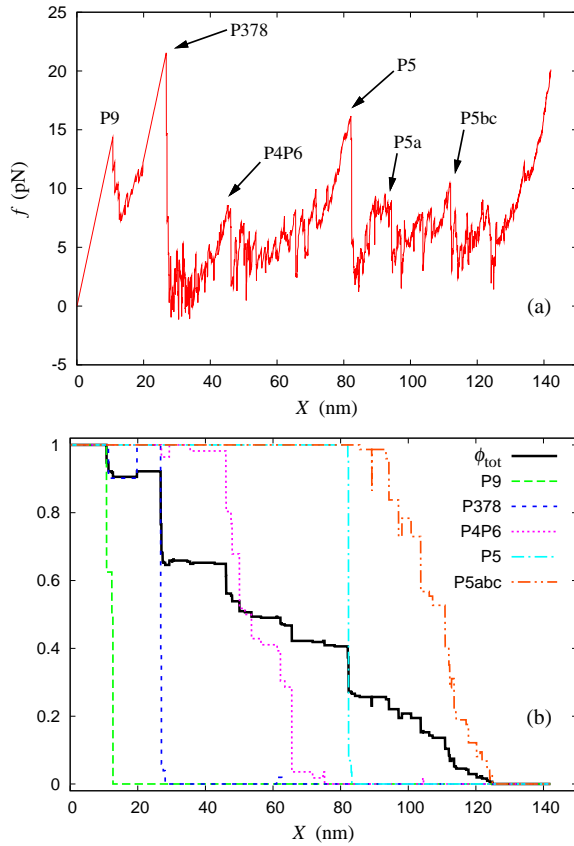


Figure 5: (Color online) Typical unfolding trajectory of the 1GRZ molecule. (a) force as a function of the position of the “optical trap” center X . (b) order parameter of the whole system and of the single SSEs as functions of X .

with the drops in the SSEs order parameters in fig. 5(b), we can associate peaks in fig. 5(a) to the unfolding of SSEs. The equilibrium behaviour of these order parameters is reported and discussed in [12]. The unfolding pathways corresponding to the 1000 trajectories can be easily clustered into two big sets. The first set (622 trajectories) corresponds to the pathway $P9 \rightarrow P34678 \rightarrow P5 \rightarrow P5a \rightarrow P5bc$. This means that P9 is the first SSE to unfold, followed by the SSEs P3, P4, P6, P7 and P8 with no definite order among them, and so on. This is consistent with the experimental pathway [3] $P9 \rightarrow P378 \rightarrow P46 \rightarrow P5 \rightarrow P5abc$, except for lumping together P378 and P46 and for splitting P5abc. This set of trajectories can be analyzed in more detail, looking for finer subdivisions, and one finds that 429 out of these 622 trajectories correspond to the pathway $P9 \rightarrow P78 \rightarrow P3 \rightarrow P46 \rightarrow P5 \rightarrow P5a \rightarrow P5bc$. Even at this finer level our results are consistent with the experimental ones [3], and we can also predict a definite order of unfolding events within the domains P378 and P5abc. Moreover, we find an alternative, less probable (355 trajectories out of 1000) pathway, $P9 \rightarrow P3 \rightarrow P46 \rightarrow P5 \rightarrow P5a \rightarrow P5bc \rightarrow P78$, where P78 are the last domains to unfold. The order of the unfold-

ing events does not appear to be affected by moderate variations of the threshold δ used to obtain the model interaction parameters ϵ_{ij} [12]. It is worth to note that such parameters take implicitly into account the effect of counterions on the stability of the native structure, see same reference.

To summarize, the present model turns out to be able to provide the equilibrium properties of an RNA hairpin with minimal computational efforts in comparison with more detailed molecular models. This feature allows us to extend our investigation to the equilibrium properties of a large molecule, namely the Tetrahymena thermophila ribozyme. The model is also able to reproduce the experimental behaviour of the ribozyme under mechanical loading, providing additional information on the unfolding events at a microscopic level not accessible to experiments, similarly to what obtained for the analysis of protein unfolding [10]. These results clearly indicate that such a model captures the basic universal features underlying the mechanical unfolding of biopolymers.

* Electronic address: imparato@phys.au.dk

† Electronic address: alessandro.pelizzola@polito.it

‡ Electronic address: marco.zamparo@pd.infn.it; Present address: Dipartimento di Fisica G. Galilei and CNISM, Università di Padova, v. Marzolo 8, Padova, Italy

- [1] J. A. Doudna and T. R. Cech, *Nature* **418**, 222 (2002).
- [2] J. Liphardt *et al*, *Science* **292**, 733 (2001).
- [3] B. Onoa *et al*, *Science* **299**, 1892 (2003).
- [4] M. Müller, F. Krzakala, M. Mézard, *Eur. Phys. J. E* **9**, 67 (2002); S. Cocco, J.F. Marko, R. Monasson, *Eur. Phys. J. E* **100**, 153 (2003); U. Gerland, R. Bundschuh, T. Hwa, *Biophys. J.* **84**, 2831 (2003); A. Imparato, L. Peliti, *Eur. Phys. J. B* **39**, 357 (2004).
- [5] C. Hyeon and D. Thirumalai, *Proc. Natl. Acad. Sci. U.S.A.* **102**, 6789 (2005).
- [6] C. Hyeon, R. I. Dima, and D. Thirumalai, *Structure* **14**, 1633 (2006).
- [7] C. Hyeon and D. Thirumalai, *Biophysical Journal* **92**, 731 (2007).
- [8] C. Hyeon, G. Morrison, and D. Thirumalai, *Proc. Natl. Acad. Sci. U.S.A.* **105**, 9604 (2008).
- [9] A. Imparato, A. Pelizzola and M. Zamparo, *Phys. Rev. Lett.* **98**, 148102 (2007); A. Imparato, A. Pelizzola and M. Zamparo, *J. Chem. Phys.* **127**, 145105 (2007).
- [10] A. Imparato and A. Pelizzola, *Phys. Rev. Lett.* **100**, 158104 (2008).
- [11] H. Wako and N. Saitô, *J. Phys. Soc. Jpn* **44**, 1931 (1978); H. Wako and N. Saitô, *ibid.* **44**, 1939 (1978); V. Muñoz *et al.*, *Nature* **390**, 196 (1997); V. Muñoz *et al.* *Proc. Natl. Acad. Sci. USA* **95**, 5872 (1998); V. Muñoz and W.A. Eaton, *ibid.* **96**, 11311 (1999); P. Bruscolini and A. Pelizzola, *Phys. Rev. Lett.* **88**, 258101 (2002).
- [12] In this appendix we (1) report the secondary structures of the RNA fragments that we have studied, (2) study the equilibrium order parameters as functions of the molecular elongation, for comparison with our nonequilibrium simulations, (3) report nonequilibrium unfolding simula-

tions of molecule 1EOR, and (4) study the effect of the cutoff distance used to define contacts on the 1GRZ unfolding nonequilibrium simulations.

- [13] B. L. Golden, A. R. Gooding, E. R. Podell, and T. R. Cech, *Science* **282**, 259 (1998).

Appendix to “Equilibrium properties and force-driven unfolding pathways of RNA molecules”

MOLECULAR STRUCTURES

In this section we report the secondary structures of the RNA fragments we have studied with our model.

In fig. A.6 we report the secondary structure of the simple hairpin P5GA (pdb code 1EOR).

In addition, in fig. A.7 we report the secondary structure of the main structured portion of the Tetrahymena thermophila ribozyme (pdb code 1GRZ). This is the portion we have considered in our work and goes from base 96 to 331, according to the pdb numbering. In the figure, the numbers which are adjacent to bases correspond to the pdb numbering, and the labeling of hairpins follows [13], where the secondary structure of the whole molecule can be found. It is worth to note, that in that work the authors obtained crystals of the ribozyme by freezing solutions containing 50 mM of MgCl_2 . This concentration is compatible with the experimental conditions of, e.g., [2, 3]. Thus, the native structure, as given in the protein data base PDB, is affected by the presence of ions Mg^{2+} , which stabilize the long range, tertiary contacts. As discussed in the text, in generating our model interaction energies ϵ_{ij} , we take into account those atom pairs whose distance is smaller than a threshold distance. Thus the effect of the Mg^{2+} ions is implicitly taken into account in our model. It is commonly believed [2,3] that tertiary contacts are bottlenecks for the molecular unfolding, which manifest as peaks in the force-extension curve, like those in fig.5a of the main text.

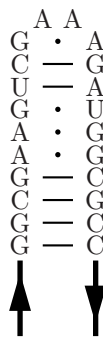


Figure A.6: Secondary structure of 1EOR

COMPARISON OF THE OUT-OF-EQUILIBRIUM UNFOLDING PATHWAYS WITH THE EQUILIBRIUM CONFIGURATIONS

In fig. A.8 the order parameter ϕ as a function of the molecular elongation L , at $T = 300$ K. Inspection of this curve suggests that at such a temperature, P9 is partially unfolded, and as the molecular elongation increases, the unfolding of P3, P4, P6, P7, and P8 start at $L = 6$ nm, the unfolding of P4 and P9 being slower than the others. At $L = 65$ nm, the P3, P6, P7 and P8 are completely unfolded, while the curves for P4 and P9 exhibits a shoulder. At the same value of the elongation, the SSEs P5, P5a, P5b, and P5c start to unfold too, and for $L \simeq 115$ nm only a small fraction of P9 and of P5abc is not yet unfolded. Such a figure has to be compared with fig. 4 and fig. 5 in the main text. The picture emerging is consistent with the typical unfolding pathways found during the simulations: $\text{P9} \rightarrow \text{P34678} \rightarrow \text{P5} \rightarrow \text{P5a} \rightarrow \text{P5bc}$. It is worth to note, however, that in out-of-equilibrium pulling manipulations the unfolding is a stochastic process, and thus the sequence of the unfolding events may vary from one realization of the process to another. For example in fig 5.b in the main text one clearly distinguish the unfolding events of P378 and P4P6, while in the equilibrium picture, fig. A.8, the unfolding of those elements occurs at almost the same length. Similarly, the characteristic lengths emerging from analysis of fig. A.8, i.e. $L = 6, 65$ nm correspond to minima in the energy landscape plotted in the inset of fig. 4 in the main text, suggesting that those minima correspond to the typical configurations of the molecule immediately before the unfolding of a specific group of SSEs.

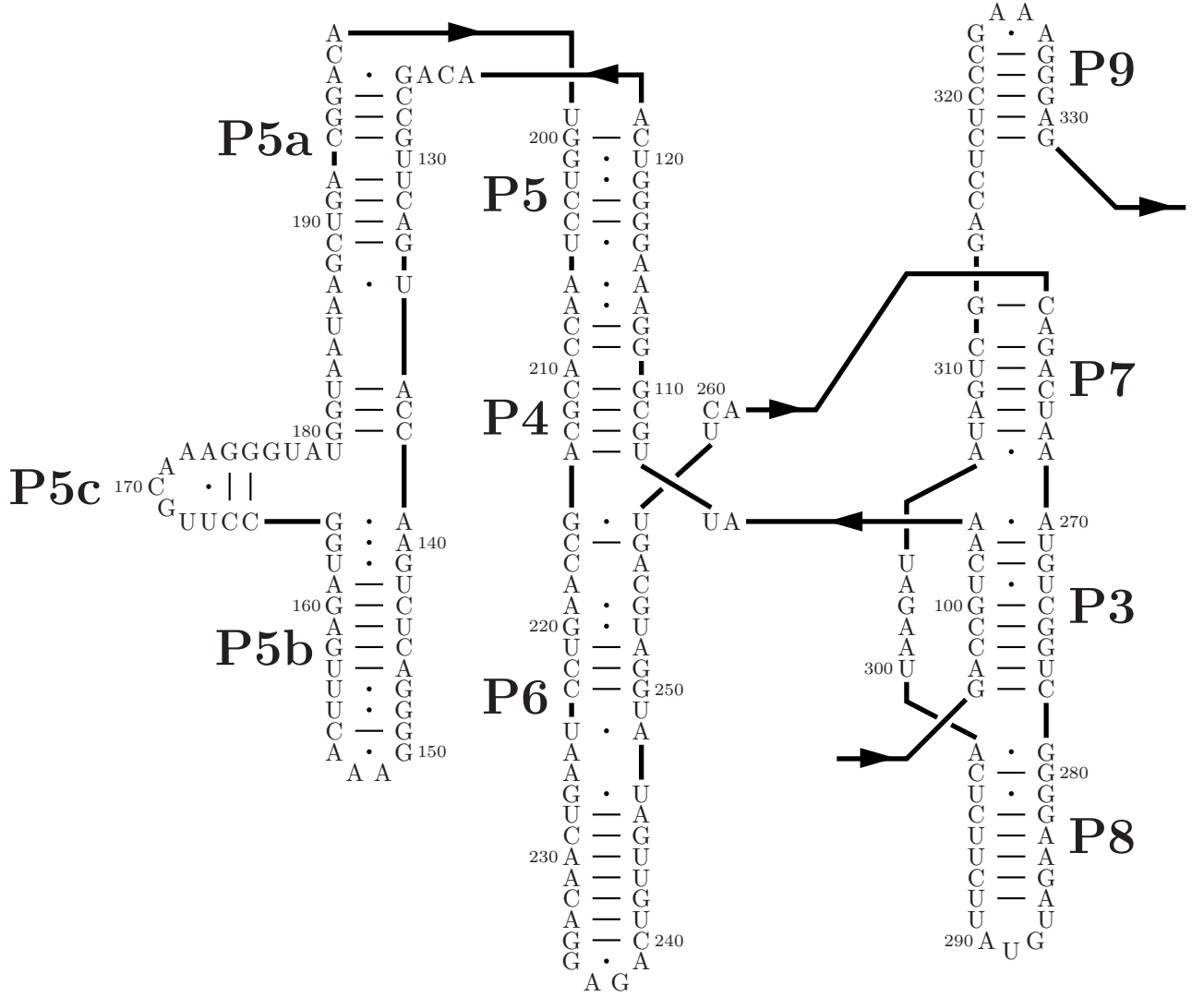


Figure A.7: Secondary structure of 1GRZ

SUPPLEMENTARY SIMULATIONS

1EOR

Here, we describe unfolding simulations of the 1EOR molecule. We consider first the constant force setup (force clamp): a constant force $f = 15.4$ pN is applied to the molecule, and its length is traced as a function of time. A typical trajectory is plotted in fig. A.9. Inspection of this figure clearly indicates that the molecule hops back and forth between two states characterized by $L \simeq 4$ nm and $L \simeq 10$ nm, which correspond to the two minima in the energy landscape of the molecule, see inset of fig. 2 in the main text.

We now consider the dynamic-loading set up. As in the main text, the force applied changes as a function of time as $f(t) = k(X(t) - L(t))$, where $L(t)$ is the end-to end length of the molecule at time t , while k and $X(t) = r \cdot t$ are the stiffness and the center of the external potential, respectively. We take the values $k = 13$ pN/nm, and $r = 1$ nm/(MC step). We find that the molecule unfolds exhibiting a peak in the force-elongation curve, at $f \simeq 12$ pN, in very good agreement with ref. [2].

1GRZ

As stated in the main text, in the present RNA model, bases i and $j + 1$ are considered to be in contact if at least two atoms, one from each base, are closer than $\delta = 4$ Å. We now study the possible effects of the threshold δ on the unfolding pathway, and in particular on the force-elongation curve.

We consider the values $\delta = 3.5, 4.5, 8$ Å, and run unfolding simulations as those described in the main text. Typical

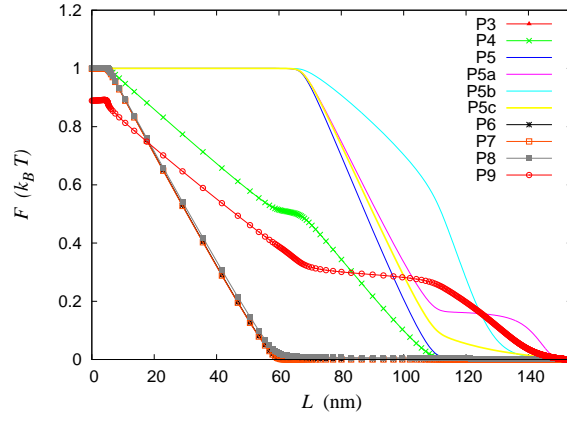


Figure A.8: Equilibrium order parameter ϕ as a function of the equilibrium molecular elongation L , at $T = 300$ K.

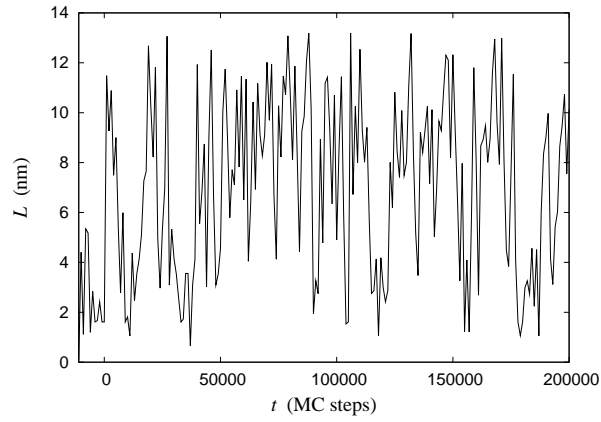


Figure A.9: Typical unfolding trajectory of the 1EOR molecule at $T = 300$ K, under constant force.

trajectories are plotted in fig. A.11: inspection of these figures suggests that increasing δ has no net effect on the unfolding pathway, the typical unfolding sequence being that of fig. 5 in the main text. For $\delta = 3.5$ however, the peaks in the force-extension curve appear to be flattened out, as one would expect, because of the reduced number and intensity of contact interactions.

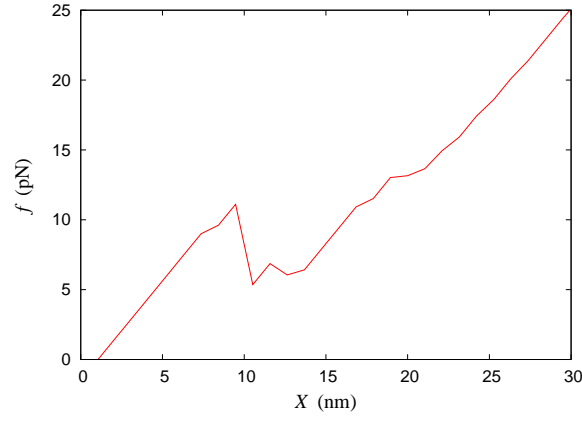


Figure A.10: Typical unfolding trajectory of the 1EOR molecule at $T = 300$ K, under time-varying force. X is the position of the center of the external quadratic potential.

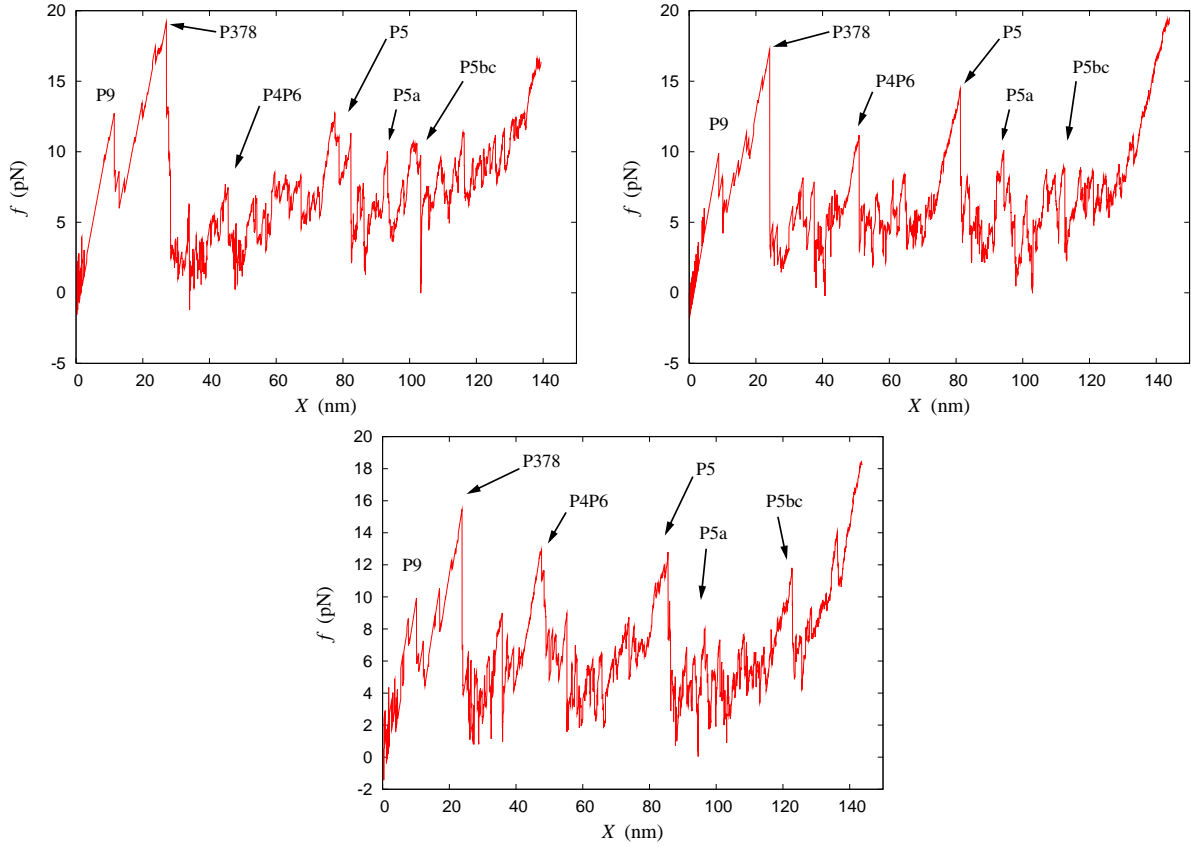


Figure A.11: Typical unfolding trajectory of the 1GRZ molecule with modified interaction parameters ϵ_{ij} . The parameters have been obtained with $\delta = 3.5$ (a), 4.5 (b) and 8 (c) Å.